Proceedings of the 17th World Congress
The International Federation of Automatic Control
Seoul, Korea, July 6-11, 2008

Fault Diagnosis Strategies for a Simulated Nonlinear Aircraft Model

M. Benini * M. Bonfè *,[1] P. Castaldi ** W. Geri ** S. Simani *

* *Department of Engineering - University of Ferrara*
Via Saragat 1, 44100 Ferrara, Italy
E-mail: {marcello.bonfe,silvio.simani}@unife.it
** *Aerospace Engineering Faculty - University of Bologna*
Via Fontanelle 40, 40136 Forlì, Italy
E-mail: {pcastaldi,wgeri}@deis.unibo.it

Abstract: In this work, different procedures for sensor Fault Detection and Isolation (FDI) applied to a simulated model of a commercial aircraft are presented. The main point of the paper regards the design of two FDI schemes based on a linear Polynomial Method (PM) and the NonLinear Geometric Approach (NLGA). The obtained results highlight a good trade–off between solution complexity and achieved performances. The FDI schemes are applied to the aircraft model, characterised by tight–coupled longitudinal and lateral dynamics. The properties of the residual generators are experimentally investigated and verified by simulating a general aircraft reference trajectory. The overall performance of the developed FDI schemes are analysed in the presence of turbulence, measurement and model errors. Comparisons with other FDI methods based on Neural Networks (NN) and Unknown Input Kalman Filter (UIKF) are finally reported.

1. INTRODUCTION

Increasing demands on reliability for safety critical systems such as aircraft require reliable control and fault diagnosis capabilities as these systems are potentially subjected to unexpected anomalies and faults in actuators, input–output sensors, components or subsystems. Consequently, fault diagnosis capabilities and requirements for aircraft applications have recently been receiving a great deal of attention in the research community (Marcos et al. (2005); Amato et al. (2006)). Development of appropriate techniques and solutions are known as the Fault Detection and Isolation (FDI) problem. There are, broadly speaking, two main approaches for addressing the FDI problem, namely hardware–based and model–based techniques (Chen and Patton (1999); Patton et al. (2000); Isermann (2005)).

A common and important approach in model–based techniques is known as the residual–based method. A crucial issue with any FDI scheme is its robustness properties. The robustness problem in FDI is defined as the maximisation of the detectability and isolability of faults together with the minimisation of the effects of uncertainty and disturbances on the FDI procedure (Chen and Patton (1999); Isermann (2005)). However, many FDI techniques are developed for linear systems. Unfortunately, practical models in real world are mostly nonlinear. Therefore, a viable procedure for practical application of FDI techniques is really necessary. Moreover, robust FDI for the case of aircraft systems and applications is still an open problem for further research.

This work deals with the residual generator design for the FDI of input–output sensors of a general aviation aircraft subject to turbulence, wind gust disturbances and measurement noises. The developed PM scheme belongs to the parity space approach (Gertler (1998)) and it is based on an input–output polynomial description of the system under diagnosis. In this way, the design of disturbance decoupled residual generators can be reduced to the determination of the null–space of a specific polynomial matrix associated to the process model. On the other hand, the development of NLGA methodology is based on the works by De Persis and Isidori (De Persis and Isidori (2000, 2001)).

It is worth noting that a previous work by the same authors (Bonfè et al. (2006)) described the design of residual generators based on the NLGA for only the longitudinal dynamics, *i.e.* the 3 Degrees of Freedom (DoF) aircraft model of the general aviation aircraft. This paper presents further investigations regarding the design of the FDI schemes for an aircraft model described as a 6 DoF rigid body. Moreover, a new fully analytical mixed $\mathcal{H}_-/\mathcal{H}_\infty$ optimisation is proposed, in order to design the residual generators so that a good trade–off between the fault sensitivity and the properties with respect to measurements and model errors is achieved. Therefore, this paper investigates some design issues and provides the FDI residual generator optimal parameters, not described in (Bonfè et al. (2006, 2007)).

The designed residual generators have been tested on a PIPER PA–30 aircraft flight simulator, that was implemented in Matlab® – Simulink® environments. Comparisons with different disturbance decoupling methods for FDI based on Neural Networks (NN) and Unknown Input Kalman Filter (UIKF) have been also provided.

[1] Corresponding author

2. AIRCRAFT MODEL

The description of the monitored aircraft and its mathematical description are recalled in this section. The main parameters and measured variables are reported in Table 1. The considered aircraft simulation model consists of a PIPER PA–30, based on the classical nonlinear 6 DoF rigid body formulation (Stevens and Lewis (2003)), whose motion occurs as a consequence of applied forces and moments (aerodynamic, propulsive and gravitational). A set of local approximations for these forces has been computed and scheduled depending on the values assumed by True Air Speed (TAS), curvature radius, flight path angle, altitude and flap deflection. In this way, it is possible to obtain a mathematical model for each flight condition. This model is suitable for a state–space representation, as it can be made explicit. The parameters in the analytic representation of the aerodynamic actions have been obtained from wind tunnel experimental data, and the aerodynamic actions are expressed along the axes of the wind reference system.

Table 1. Aircraft model nomenclature.

V	True Air Speed (TAS)
α	angle of attack
β	angle of sideslip
p_ω	roll rate
q_ω	pitch rate
r_ω	yaw rate
ϕ	bank angle
θ	elevation angle
ψ	heading angle
n_e	engine shaft angular rate
$\begin{bmatrix} I_x & 0 & -I_{xz} \\ 0 & I_y & 0 \\ -I_{xz} & 0 & I_z \end{bmatrix}$	inertia moment matrix
F_x, F_y, F_z	body axes forces
M_x, M_y, M_z	body axes moments
δ_e	elevator deflection angle
δ_a	aileron deflection angle
δ_r	rudder deflection angle
δ_{th}	throttle aperture percentage
X, Y	horizontal coordinates
H	altitude
γ	flight path angle
m	airplane mass
ω_u, ω_v, ω_w	wind gust components

The nonlinear 6 DoF model has been completed by means of the PIPER PA–30 propulsion system consisting of two 4–pistons aspirated engines, with the throttle valve aperture δ_{th} as input and the overall thrust intensity as output. Thus, the complete simulation model consists of the aircraft 6 DoF flight dynamics and the engine model completed with the model of input–output sensors, the servo actuators, the atmosphere turbulence Dryden description, the wind gust disturbances and a classical autopilot. Moreover, the sensor models embed all the possible sources of disturbance (calibration and alignment errors, scale factor, white and coloured noises, limited bandwidth, g–sensitivity, gyro drift, *etc.*).

Using the nomenclature of Table 1, it is possible to develop the nonlinear model mathematical equations for the aircraft flight attitude (Bonfè et al. (2006, 2007)). The linear model used by the proposed PM FDI approach described in Section 4 is obtained from the linearisation of both the 6 DoF model and the propulsion system as follows:

$$\dot{x}(t) = \mathbf{A}\, x(t) + \mathbf{B}\, c(t) + \mathbf{E}\, d(t) \tag{1}$$

with

$$\begin{aligned} x(t) &= \big[\Delta V(t)\ \ \Delta\alpha(t)\ \ \Delta\beta(t)\ \ \Delta p_\omega(t)\ \ \Delta q_\omega(t)\ \dots \\ &\qquad \dots\ \Delta r_\omega(t)\, \Delta\phi(t)\ \ \Delta\theta(t)\ \ \Delta\psi(t)\ \ \Delta n_e(t)\big]^T \\ c(t) &= \big[\Delta\delta_e(t)\ \ \Delta\delta_a(t)\ \ \Delta\delta_r(t)\ \ \Delta\delta_{th}(t)\big]^T \\ d(t) &= \big[w_u(t)\ \ w_v(t)\ \ w_w(t)\big]^T \end{aligned} \tag{2}$$

where Δ denotes the variations of the considered variables, while $c(t)$ and $d(t)$ are the control inputs and the disturbances respectively. The disturbance contribution of the wind gusts as air velocity components, w_u, w_v and w_w, along body axes was also considered. The output equation associated to the model (1) is of the type $y(t) = \mathbf{C}\, x(t)$, where the rows of $\mathbf{C}$ correspond to rows of the identity matrix, depending on the measured variables.

With reference to the NLGA FDI scheme described in Section 3, it requires a nonlinear input affine system (De Persis and Isidori (2001)), but the adopted simulation model of the aircraft does not fulfil this requirement. For this reason, the following simplified aircraft model is used:

$$\left\{ \begin{aligned} \dot{V} &= -\frac{\left(C_{D0} + C_{D\alpha}\alpha + C_{D\alpha_2}\alpha^2\right)}{m} V^2 + \\ &\quad + g\left(\sin\alpha\cos\theta\cos\phi - \cos\alpha\sin\theta\right) + \\ &\quad + \frac{\cos\alpha}{m}\frac{t_p}{V}\left(t_0 + t_1 n_e\right)\delta_{th} + w_v \sin\alpha \\ \dot{\alpha} &= -\frac{\left(C_{L0} + C_{L\alpha}\alpha\right)}{m} V + \\ &\quad + \frac{g}{V}\left(\cos\alpha\cos\theta\cos\phi + \sin\alpha\sin\theta\right) + q_\omega + \\ &\quad - \frac{\sin\alpha}{m}\frac{t_p}{V^2}\left(t_0 + t_1 n_e\right)\delta_{th} + \frac{\cos\alpha}{V} w_v \\ \dot{\beta} &= \frac{\left(C_{D0} + C_{D\alpha}\alpha + C_{D\alpha_2}\alpha^2\right)\sin\beta + C_{Y\,\beta}\beta\cos\beta}{m} V + \\ &\quad + g\frac{\cos\theta\sin\phi}{V} + p_\omega\sin\alpha - r_\omega\cos\alpha + \\ &\quad - \frac{\cos\alpha\sin\beta}{m}\frac{t_p}{V^2}\left(t_0 + t_1 n_e\right)\delta_{th} + \frac{1}{V} w_\ell \\ \dot{p}_\omega &= \frac{\left(C_{l\beta}\beta + C_{lp}\, p_\omega\right)}{I_x} V^2 + \frac{(I_y - I_z)}{I_x} q_\omega r_\omega + \frac{C_{\delta_a}}{I_x} V^2 \delta_a \\ \dot{q}_\omega &= \frac{\left(C_{m0} + C_{m\alpha}\alpha + C_{mq}\, q_\omega\right)}{I_y} V^2 + \frac{(I_z - I_x)}{I_y} p_\omega r_\omega + \\ &\quad + \frac{C_{\delta_e}}{I_y} V^2 \delta_e + \frac{t_d}{I_y}\frac{t_p}{V}\left(t_0 + t_1 n_e\right)\delta_{th} \\ \dot{r}_\omega &= \frac{\left(C_{n\beta}\beta + C_{nr}\, r_\omega\right)}{I_z} V^2 + \frac{(I_x - I_y)}{I_z} p_\omega q_\omega + \frac{C_{\delta_r}}{I_z} V^2 \delta_r \\ \dot{\phi} &= p_\omega + \left(q_\omega\sin\phi + r_\omega\cos\phi\right)\tan\theta \\ \dot{\theta} &= q_\omega\cos\phi - r_\omega\sin\phi \\ \dot{\psi} &= \frac{\left(q_\omega\sin\phi + r_\omega\cos\phi\right)}{\cos\theta} \\ \dot{n}_e &= t_n n_e^3 + \frac{t_f}{n_e}\left(t_0 + t_1 n_e\right)\delta_{th} \end{aligned} \right. \tag{3}$$

where $C_{(\cdot)}$ are the aerodynamic coefficients; $t_{(\cdot)}$ are the engine parameters; w_v, w_l are the vertical and lateral wind disturbance components. In more detail, the model of Eq. (3) has been obtained by assuming that the expressions of aerodynamic forces and moments can be represented by means of series expansions in the neighbourhood of the steady–state flight condition. The engine model has been simplified by linearising the power with respect to the angular rate behaviour in the neighbourhood of the trim point. The second order coupling between the longitudinal and lateral–directional dynamics have been neglected. The x–body axis component of the wind has been neglected. In fact, the aircraft behaviour is much more sensitive to the y–body and z–body axis wind components. The rudder effect in the equation describing the β dynamics has been neglected.

3. NLGA RESIDUAL GENERATORS

The considered NLGA to the FDI problem was formally developed in (De Persis and Isidori (2001)). It consists in finding, by means of a coordinate change in the state space and in the output space, an observable subsystem which, if possible, is affected by the fault and not affected by disturbances. In this way, necessary and sufficient conditions for the FDI problem to be solvable are given. Finally, a residual generator can be designed on the basis of the model of the observable subsystem. More precisely, the approach consider a nonlinear system model in the form:

$$\begin{cases} \dot{x} &= n(x) + g(x)\,c(t) + \ell(x)\,f(t) + p(x)\,d(t) \\ y(t) &= h(x) \end{cases} \tag{4}$$

in which the state vector $x \in \mathcal{X}$ (an open subset of $\mathcal{R}^n$), $c(t) \in \mathcal{R}^{\ell_c}$ is the control input vector, $f(t) \in \mathcal{R}^{\ell_f}$ is the fault vector, $d(t) \in \mathcal{R}^{\ell_d}$ the disturbance vector and $y \in \mathcal{R}^m$ the output vector, whilst $n(x)$, $g(x)$, $\ell(x)$ and $p(x)$ are smooth vector fields, and $h(x)$ a smooth map. Therefore, if P represents the distribution spanned by the column of $p(x)$, the NLGA method is based firstly on the determination the largest observability codistribution contained in $P^{\perp}$, denoted with Ω^* (De Persis and Isidori (2001)).

If $\ell(x) \in \Omega^*$, the fault is not detectable. Otherwise, the design procedure is possible and it can be found a surjection Ψ_1 and a function Φ_1 fulfilling $\Omega^* \cap \text{span}\{dh\} = \text{span}\{d(\Psi_1 \circ h)\}$ and $\Omega^* = \text{span}\{d(\Phi_1)\}$, respectively.

The functions $\Psi(y)$ and $\Phi(x)$ defined as:

$$\Psi(y) = \begin{pmatrix} \bar{y}_1 \\ \bar{y}_2 \end{pmatrix} = \begin{pmatrix} \Psi_1(y) \\ H_2\, y \end{pmatrix},$$

and

$$\Phi(x) = \begin{pmatrix} \bar{x}_1 \\ \bar{x}_2 \\ \bar{x}_3 \end{pmatrix} = \begin{pmatrix} \Phi_1(x) \\ H_2\, h(x) \\ \Phi_3(x) \end{pmatrix}$$

are (local) diffeomorphisms. In the new (local) coordinate defined previously, the system of Eq. (4) is described by the relations in the form:

$$\begin{cases} \dot{\bar{x}}_1 = n_1(\bar{x}_1, \bar{x}_2) + g_1(\bar{x}_1, \bar{x}_2)\,c + \ell_1(\bar{x}_1, \bar{x}_2, \bar{x}_3)\,f \\ \dot{\bar{x}}_2 = n_2(\bar{x}_1, \bar{x}_2, \bar{x}_3) + g_2(\bar{x}_1, \bar{x}_2, \bar{x}_3)\,c + \\ \qquad + \ell_2(\bar{x}_1, \bar{x}_2, \bar{x}_3)\,f + p_2(\bar{x}_1, \bar{x}_2, \bar{x}_3)\,d \\ \dot{\bar{x}}_3 = n_3(\bar{x}_1, \bar{x}_2, \bar{x}_3) + g_3(\bar{x}_1, \bar{x}_2, \bar{x}_3)\,c + \\ \qquad + \ell_3(\bar{x}_1, \bar{x}_2, \bar{x}_3)\,f + p_3(\bar{x}_1, \bar{x}_2, \bar{x}_3)\,d \\ \bar{y}_1 = h(\bar{x}_1) \\ \bar{y}_2 = \bar{x}_2 \end{cases} \tag{5}$$

with $\ell_1(\bar{x}_1, \bar{x}_2, \bar{x}_3)$ not identically zero. Denoting $\bar{x}_2$ with $\bar{y}_2$ and considering it as an independent input, it can be singled out the $\bar{x}_1$–subsystem:

$$\begin{cases} \dot{\bar{x}}_1 = f_1(\bar{x}_1, \bar{y}_2) + g_1(\bar{x}_1, \bar{y}_2)\,c + \ell_1(\bar{x}_1, \bar{y}_2, \bar{x}_3)\,m \\ \bar{y}_1 = h(\bar{x}_1) \end{cases}$$

which is affected by the fault and decoupled from the disturbance. This subsystem has been exploited for the design of the residual generator for the FDI of the fault f.

With reference to the considered aircraft application, as can be seen in (Castaldi et al. (2007)), it is always possible to find two proper scalar components both of $\bar{x}_1$ and $\bar{y}_1$, referred to as $\bar{x}_{11}$ and $\bar{y}_{11}$, so that the following $\bar{x}_{11}$–subsystem can be singled out:

$$\begin{cases} \dot{\bar{x}}_{11} = n_{11}(\bar{x}_{11}, \bar{y}_{1c}, \bar{y}_2) + g_{11}(\bar{x}_{11}, \bar{y}_{1c}, \bar{y}_2)c + \\ \qquad + \ell_{11}(\bar{x}_{11}, \bar{y}_{1c}, \bar{y}_2)f \\ \bar{y}_{11} = \bar{x}_{11} \end{cases} \tag{6}$$

where

$$\bar{x}_1 = \begin{bmatrix} \bar{x}_{11} \\ \bar{x}_{1c} \end{bmatrix} \qquad \bar{y}_1 = \begin{bmatrix} \bar{y}_{11} \\ \bar{y}_{1c} \end{bmatrix}$$

The generic adopted scalar residual generator for the fault detection of the $\bar{x}_{11}$–subsystem (6) can be written as:

$$\begin{cases} \dot{\xi}_f = n_{11}(\bar{y}_{11}, \bar{y}_{1c}, \bar{y}_2) + g_{11}(\bar{y}_{11}, \bar{y}_{1c}, \bar{y}_2)c + k_f\,(\bar{y}_{11} - \xi_f) \\ r_f = \bar{y}_{11} - \xi_f \end{cases} \tag{7}$$

As an example, the residual generator signal $r_{\delta_e}(t)$ for the elevator of the input affine model of Eq. (3), with $k_{\delta_e} > 0$ to ensure asymptotic stability, is described by the relation:

$$\begin{cases} \dot{\xi}_1 = \dfrac{V^2}{m}\left[-\left(C_{D0} + C_{D\alpha}\alpha + C_{D\alpha_2}\alpha^2\right)\cos\alpha\right] + \\ \quad + \dfrac{V^2}{m}\left(C_{L0} + C_{L\alpha}\alpha\right)\sin\alpha - g\sin\theta + \\ \quad - V\,q_\omega \sin\alpha - \dfrac{(C_{m0} + C_{m\alpha}\alpha + C_{mq}q_\omega)}{m t_d} V^2 + \\ \quad - \dfrac{(I_z - I_x)}{m t_d} p_\omega r_\omega - \dfrac{C_{\delta_e}}{m t_d} V^2 \delta_e + \\ \quad + k_{\delta_e}\left[\left(V\cos\alpha - \dfrac{I_y}{m t_d} q_\omega\right) - \xi_1\right] \\ r_{\delta_e} = \left(V\cos\alpha - \dfrac{I_y}{m t_d} q_\omega\right) - \xi_1 \end{cases} \tag{8}$$

The residual generators for the aileron $r_{\delta_a}(t)$, the rudder $r_{\delta_r}(t)$ and the throttle $r_{\delta_{th}}(t)$ input sensor signals have similar formulations and they are not reported here. The design of the residual generator gains k_{δ_e}, k_{δ_a}, k_{δ_r} and $k_{\delta_{th}}$ can be carried out independently.

It can be noted that the critical disturbances are previously structurally decoupled but there are some other non critical disturbance affecting both the aircraft dynamics and the sensor measurements which has to be considered in order to improve the robustness of the fault detection. For this reason, the tuning of the generic residual generator gain k_f will be performed by embedding the description of the non critical disturbances in the $\bar{x}_{11}$–subsystem as follows:

$$\begin{cases} \dot{\bar{x}}_{11} = n_{11}(\bar{x}_{11}, \bar{y}_{1c}, \bar{y}_2) + g_{11}(\bar{x}_{11}, \bar{y}_{1c}, \bar{y}_2)c + \\ \qquad + \ell_{11}(\bar{x}_{11}, \bar{y}_{1c}, \bar{y}_2)f + e(\bar{x}_{11}, \bar{y}_{1c}, \bar{y}_2)\zeta \\ \bar{y}_{11} = \bar{x}_{11} + \nu \end{cases} \tag{9}$$

where the variable $\nu \in \mathcal{R}$ is the measurement noise on $\bar{x}_{11}$, the variable $\zeta \in \mathcal{R}$ and the related scalar field $e(\cdot)$ represent the non critical effects which have not been explicitly considered in the aircraft model (3).

A procedure for optimising the trade–off between the fault, the modelling error and disturbance sensitivity of the generic residual generator is proposed in the following. In more detail, in order to take into account the disturbance attenuation and fault sensitivity, the mixed $\mathcal{H}_-/\mathcal{H}_\infty$ approach is exploited (Chen and Patton (1999); Hou and Patton (1996)).

In order to determine a new analytic solution to the mixed $\mathcal{H}_-/\mathcal{H}_\infty$ problem, aimed to tune the generic k_f of the non linear residual generator, the dynamics of the estimation error can be linearised since the considered aircraft application is characterised by small excursions of the state, input and output variables with respect to their trim values. The estimation error is defined as follows:

$$\tilde{x}_f = \bar{x}_{11} - \xi_f \tag{10}$$

and the corresponding linearised dynamics is represented by:

$$\begin{cases} \dot{\tilde{x}}_f &= -k_f\,\tilde{x}_f + (E_1 - k_f E_2)\,\varepsilon + m f \\ r_f &= \tilde{x}_f + E_2\varepsilon \end{cases} \tag{11}$$

where the disturbance augmented vector ε and the corresponding E_1, E_2 are structurally defined as:

$$\varepsilon = \begin{bmatrix} \zeta \\ \nu \end{bmatrix} \qquad E_1 = [e_{11}\ 0] \qquad E_2 = [0\ 1] \tag{12}$$

¿From the definitions of the norms $\mathcal{H}_\infty$ and $\mathcal{H}_-$ for a stable transfer function G (Chen and Patton (1999)), the mixed $\mathcal{H}_-/\mathcal{H}_\infty$ residual optimisation problem is stated as follows.

Given two scalars $\beta > 0$ and $\gamma > 0$, find the set $\mathcal{K}$ defined as:

$$\mathcal{K} = \left\{ k_f \in \mathcal{R} :\ k_f > 0,\ \|G_{r\varepsilon}\|_\infty < \gamma,\ \|G_{rf}\|_- > \beta \right\} \tag{13}$$

where

$$G_{r\,\varepsilon}(s) = (s + k_f)^{-1}\ (E_1 - k_f\, E_2) + E_2 \tag{14}$$

$$G_{rf}(s) = (s + k_f)^{-1}\ m \tag{15}$$

It is possible to prove that for each $k_f > 0$

$$\|G_{r\varepsilon}\|_\infty^2 = \max\left\{ 1,\ \frac{e_{11}^2}{k_f^2} \right\} \tag{16}$$

Moreover, the set $\mathcal{K}_\gamma$ defined as

$$\mathcal{K}_\gamma = \{ k_f \in \mathcal{R} :\ k_f > 0,\ \|G_{r\varepsilon}\|_\infty < \gamma,\ \gamma > 1 \} \tag{17}$$

is given by:

$$k_f > \underline{k} \quad \textit{with} \quad \underline{k} = \frac{e_{11}}{\gamma} \tag{18}$$

On the other hand, the set $\left\{ \|G_{rf}\|_- :\ \|G_{r\varepsilon}\|_\infty < \gamma \right\}$, with $\gamma > 1$, is given by:

$$0 < \|G_{rf}\|_- < \beta_{\max}(\gamma) \qquad \text{where} \qquad \beta_{\max}(\gamma) = \frac{m\,\gamma}{e_{11}} \tag{19}$$

By combining the previous results, it is possible to provide an analytical expression of the set $\mathcal{K}$ as follows:

$$\mathcal{K} = \left\{ k_f \in \mathcal{R} : k_f \in \left]\underline{k}\,, \overline{k}\right[,\ \underline{k} = \frac{m}{\beta_{\max}(\gamma)},\ \overline{k} = \frac{m}{\beta} \right\} \tag{20}$$

On the basis of these results, k_f can be designed by choosing a desired value of disturbance attenuation $\gamma > 1$. Then, it is required to compute $\beta_{\max}(\gamma)$ and choose $\beta \in]0,\ \beta_{\max}(\gamma)[$ to obtain a desired value of fault sensitivity. Finally, one has to choose the gain of the nonlinear residual generator $k_f \in \left]\underline{k}\,, \overline{k}\right[$.

4. PM RESIDUAL GENERATORS

The input–output representation of a continuous–time, time–invariant linear dynamic system affected by faults and disturbances is assumed to have the form:

$$\mathbf{P}(s)\,\mathbf{y}(t) = \mathbf{Q}_c(s)\,\mathbf{c}(t) + \mathbf{Q}_d(s)\,\mathbf{d}(t) + \mathbf{Q}_f(s)\,\mathbf{f}(t), \tag{21}$$

where $\mathbf{y}(t) \in \Re^m$ is the output vector, $\mathbf{c}(t) \in \Re^{l_c}$ is the input vector, $\mathbf{d}(t) \in \Re^{l_d}$ is the disturbance vector and $\mathbf{f}(t) \in \Re^{l_f}$ is the fault vector; $\mathbf{P}(s)$, $\mathbf{Q}_c(s)$, $\mathbf{Q}_d(s)$ and $\mathbf{Q}_f(s)$ are known polynomial matrices of proper dimensions.

Models of type of Eq. (21) can be frequently found in practice by applying well–known physical laws to describe the input–output dynamical links of various systems. Algorithms to transform multivariable state–space models to equivalent Multiple Input – Multiple Output (MIMO) polynomial representations and vice versa are available. Under this consideration, the polynomial matrices $\mathbf{P}(s)$, $\mathbf{Q}_c(s)$ and $\mathbf{Q}_d(s)$ can be obtained by physical modelling or black–box identification procedures, as suggested in (Chen and Patton (1999); Simani et al. (2002)) for state–space and input–output system descriptions.

An important aspect of the residual generator design for the system of Eq. (21) concerns the de–coupling properties of the disturbance $\mathbf{d}(t)$. The de–coupling can be obtained premultiplying all the terms of Eq. (21) by the matrix $\mathbf{L}(s) \in \mathcal{N}_l\,(\mathbf{Q}_d(s))$, *i.e.* the left null–space of the matrix $\mathbf{Q}_d(s)$:

$$\mathbf{L}(s)\,\mathbf{P}(s)\,\mathbf{y}(t) - \mathbf{L}(s)\,\mathbf{Q}_c(s)\,\mathbf{c}(t) = \mathbf{L}(s)\,\mathbf{Q}_f(s)\,\mathbf{f}(t). \tag{22}$$

Hence, the residual generator for the system of Eq. (21) is represented by:

$$\begin{aligned} R(s)\,r(t) &= \mathbf{L}(s)\,\mathbf{P}(s)\,\mathbf{y}(t) - \mathbf{L}(s)\,\mathbf{Q}_c(s)\,\mathbf{c}(t) = \\ &= \mathbf{L}(s)\,\mathbf{Q}_f(s)\,\mathbf{f}(t), \end{aligned} \tag{23}$$

where it is assumed that $r(t) \in \Re$ and $\mathbf{L}(s)$ is a polynomial row vector. The polynomial $R(s)$ can be arbitrarily selected among the polynomials with degree greater than or equal to n_r^*, where n_r^* is the maximum row–degree of the pair $\{\mathbf{L}(s)\,\mathbf{P}(s)\,,\,\mathbf{L}(s)\,\mathbf{Q}_c(s)\}$. Moreover, if all the roots of $R(s)$ lie in the open left–half s–plane, it assures the stability of the filter of Eq. (23).

Note that if the matrix $\mathbf{Q}_d(s)$ has full row rank (*i.e.* $\operatorname{rank}\mathbf{Q}_d(s) = l_d$), $\mathcal{N}_l(\mathbf{Q}_d(s))$ has dimension $m - l_d$. Therefore, a polynomial matrix $\mathbf{B}(s)$, whose rows represent a minimal polynomial basis of $\mathcal{N}_l\,(\mathbf{Q}_d(s))$, has $m - l_d$ rows and m columns.

As it is assumed that the input–output measurements are expressed by the following relations:

$$\begin{cases} \mathbf{c}^*(t) = \mathbf{c}(t) + \mathbf{f}_c(t), \\ \mathbf{y}^*(t) = \mathbf{y}(t) + \mathbf{f}_o(t), \end{cases} \tag{24}$$

the system of Eq. (21) becomes:

$$\begin{aligned} \mathbf{P}(s)\ (\mathbf{y}^*(t) - \mathbf{f}_o(t)) &= \mathbf{Q}_c(s)\ (\mathbf{c}^*(t) - \mathbf{f}_c(t)) + \\ &\quad + \mathbf{Q}_d(s)\,\mathbf{d}(t), \end{aligned} \tag{25}$$

whilst the residual generator of Eq. (23):

$$\begin{aligned} R(s)\,r(t) &= \mathbf{L}(s)\,\mathbf{P}(s)\,\mathbf{y}^*(t) - \mathbf{L}(s)\,\mathbf{Q}_c(s)\,\mathbf{c}^*(t) = \\ &= \mathbf{L}(s)\,\mathbf{P}(s)\,\mathbf{f}_o(t) - \mathbf{L}(s)\,\mathbf{Q}_c(s)\,\mathbf{f}_c(t). \end{aligned} \tag{26}$$

It is clear that the design freedom consists of the selection of the rows of the polynomial matrix $\mathbf{L}(s)$, when $q = m - l_d \geq 2$. These degrees of freedom are used to optimise the sensitivity properties of $r(t)$ with respect to the fault $f(t)$, for example by maximising the steady–state gain of the transfer function $G_f(s) = \mathbf{L}(s)\,\mathbf{Q}_f(s)/R(s)$.

If $\mathbf{b}_i(s)$ $(i = 1, \ldots, q)$ are the row vectors of the basis $\mathbf{B}(s)$, $\mathbf{L}(s)$ can be expressed as linear combination of these vectors:

$$\mathbf{L}(s) = \sum_{i=1}^{q} k_i\,\mathbf{b}_i(s), \tag{27}$$

where k_i are real constants maximising:

$$\lim_{s\to 0} \frac{1}{R(s)} \left[\sum_{i=1}^{q} k_i \mathbf{b}_i(s)\right] \mathbf{Q}_f(s) = \left[\sum_{i=1}^{q} k_i \mathbf{b}_i(0)\right] \mathbf{Q}_f(0), \tag{28}$$

with the constraint:

$$\sum_{i=1}^{q} {k_i}^2 = 1. \tag{29}$$

Under these assumptions, when the fault $f(t)$ is a step–function of magnitude F, the steady–state residual value is:

$$\begin{aligned} \lim_{t\to\infty} r(t) &= \lim_{s\to 0} s\,\frac{\mathbf{L}(s)\,\mathbf{Q}_f(s)}{R(s)}\,\frac{F}{s} = \\ &= \left[\sum_{i=1}^{q} k_i\,\mathbf{b}_i(0)\right] \mathbf{Q}_f(0)\,F. \end{aligned} \tag{30}$$

By defining the real vectors $\mathbf{k} = [k_1, k_2, \ldots, k_q]^T$ and $\mathbf{a} = \mathbf{B}(0)\,\mathbf{Q}_f(0) = [a_1, a_2, \ldots, a_q]$, the maximisation of the residual fault sensitivity is determined by the vector $\mathbf{k}$ that maximises the steady–state fault sensitivity, *i.e.* the function W given by $W = \mathbf{a}^T\,\mathbf{k} = \sum_{i=1}^{q} a_i\,k_i$ under the constraint of Eq. (29), given the vector $\mathbf{a}$. The solution to this problem exists and it is unique. In fact, from Eq. (29), k_1 is expressed as a function of $k_2, k_3, \ldots, k_q$ and it is substituted into the expression of the function W. Thus $W = a_1\sqrt{1 - {k_2}^2 - {k_3}^2 - \ldots - {k_q}^2} + a_2\,k_2 + \ldots + a_q\,k_q$.

By computing $\nabla W = 0$ and squaring the expression, after algebraic manipulation, an expression in the form of $\mathbf{A}\,\mathbf{x} = \mathbf{b}$ is obtained, where $\mathbf{A}$ and $\mathbf{b}$ depend on the terms ${a_i}^2$. The unknown vector $\tilde{\mathbf{x}}$, under the constraint of Eq. (29), can be expressed as $\tilde{\mathbf{x}} = [1 - \sum_{i=1}^{q-1}(\mathbf{A}^{-1}\,\mathbf{b})_i,\ \mathbf{A}^{-1}\mathbf{b}]^T$, where $(\mathbf{A}^{-1}\,\mathbf{b})_i$ is the i–th element of the vector $\mathbf{A}^{-1}\,\mathbf{b}$. The vector $\tilde{\mathbf{x}}$ represents the squares of the solution of the maximisation problem. If we define Ω as the set of the vectors $\mathbf{k}$ whose elements are the square roots of the elements of $\tilde{\mathbf{x}}$ (since every element can be taken both with signs '+' and '-', such vectors are 2^q), the solution $\tilde{\mathbf{k}}$ can be reformulated as:

$$\tilde{\mathbf{k}} = \arg\max_{\mathbf{k}\in\Omega} W(\mathbf{k}).$$

The maximisation of the steady–state gain of the transfer function $G_f(s) = \mathbf{L}(s)\,\mathbf{Q}_f(s)/R(s)$ is obtained through a suitable choice of the real vector $\mathbf{k}$. The design of the residual generation filter can be enhanced by introducing a method for assigning both the zeros and the poles of the transfer function $G_f(s)$. The previous consideration leads to introduce the polynomial $E(s) = \mathbf{k}^T(s)\,\mathbf{B}(s)\,\mathbf{Q}_f(s)$, where $\mathbf{k}(s)$ is a q–dimensional polynomial vector, whose i–th element has the form $k_i(s) = \sum_{j=0}^{n_k} k_i^j\,s^j$. The degree n_k and the $q \times n_k$ coefficients k_i^j represent a design freedom $(j \neq 0)$ that can be exploited to obtain the desired roots of the polynomial $E(s)$. However, in order to maximise the steady–state gain, the following condition must hold:

$$\mathbf{k}(0) = \tilde{\mathbf{k}} = \left[\,\tilde{k_1}\ \tilde{k_2}\ \ldots\ \tilde{k_q}\,\right]^T \tag{31}$$

where $k_i^0 = \tilde{k_i}$, with $i = 1, \ldots, q$. If $H(s)$ is the reference polynomial, whose roots are the zeros to be assigned, *i.e.* $H(s) = \sum_{j=0}^{n_h} h^j\,s^j$, it follows that $H(0) = \tilde{\mathbf{k}}^T\,\mathbf{B}(0)\,\mathbf{Q}_f(0)$. Obviously, this assumption does not provide any restriction on the roots assignable. Under the previous considerations, the zero assignment and pole placement problem can be solved by finding the degree n_k and the coefficients k_i^j, under the constraint of Eq. (31), in order to obtain $E(s) = H(s)$.

To proceed, we define the polynomial vector $\mathbf{a}(s) = \mathbf{B}(s)\,\mathbf{Q}_f(s)$ and its i–th element, a known polynomial of a certain degree, n_{a_i}. If n_a is defined as $n_a = \max_{i=1,\ldots,q} n_{a_i}$, the i–th element of $\mathbf{a}(s)$ can be always written as a polynomial of degree n_a, *i.e.* $a_i(s) = \sum_{j=0}^{n_a} a_i^j\,s^j$ by imposing that $a_i^j = 0$ when $j > n_{a_i}$. As $E(s) = \mathbf{k}^T(s)\,\mathbf{a}(s)$, it results:

$$E(s) = \sum_{i=1}^{q} \sum_{j=0}^{n_k+n_a} \left(\sum_{\alpha+\beta=j} k_i^\alpha\,a_i^\beta\right) s^j = \sum_{j=0}^{n_k+n_a} e^j\,s^j, \tag{32}$$

where

$$e^j = \sum_{i=1}^{q} \sum_{\alpha+\beta=j} k_i^\alpha\,a_i^\beta.$$

Note that the coefficients $e^1, \ldots, e^{n_k+n_a}$ depend on the design freedom $k_i^1, \ldots, k_i^{n_k}$. On the other hand, e^0 is fixed as the coefficients k_i^0 are assigned by Eq. (31).

Let's suppose that $n_h \leq n_k + n_a$. By imposing $E(s) = H(s)$, the following expressions are computed:

$$\sum_{i=1}^{q} \sum_{\alpha+\beta=j\ (\alpha\neq 0)} k_i^\alpha\,a_i^\beta = h^j - \sum_{i=1}^{q} k_i^0\,a_i^j \tag{33}$$

for $j = 1, \ldots, n_k + n_a$.

Eqs. (31) and (33) represent a linear system with $n_k + n_a$ equations and $q \times n_k$ unknowns, that can be expressed in the classical form $\mathbf{A}\,\mathbf{x} = \mathbf{b}$, where $\mathbf{A}$ and $\mathbf{b}$ are functions of a_j^i and k_i^0. The degree n_k of the polynomials $k_i(s)$ has to be chosen in order to obtain a solvable system (*i.e.* $\operatorname{rank}\mathbf{A} = \operatorname{rank}[\mathbf{A}\ \mathbf{b}]$). Note that the use of a polynomial vector $\mathbf{k}(s)$ instead of a real vector $\mathbf{k}$ has the drawback of increasing the complexity of the residual generator.

The detection properties of the filters in terms of fault sensitivity and disturbance rejection can be optimised by using a method similar to the one described in Section 3 for the NLGA residuals. In particular, the synthesis of the dynamic filters for FDI has been performed by choosing a suitable linear combination of residual generator functions. This choice maximises the steady–state gain of the transfer functions between input sensor fault signals. The roots of the $R(s)$ polynomial matrix are optimised for maximising the fault detection promptness, as well as to minimise the disturbance sensitivity.

Finally, the design problem of residual generator banks for the isolation of faults affecting the input and the output sensors can be solved by using the disturbance de–coupling method suggested above. In particular, to univocally isolate a fault concerning one of the *output sensors*, under the hypotheses that the input sensors and the remaining output sensors are fault–free, a bank of residual generator filters is used. The number of these generators is equal to the number m of the system outputs, and the i–th device ($i = 1, \ldots, m$) is driven by all but the i–th output and all the inputs of the system. In this case, a fault on the i–th output sensor affects all but the i–th residual generator. Moreover, the parameters of the i–th filter can be properly chosen in order to optimise its performances when a fault is acting on the j–th output sensor. A similar design technique can be used for *input sensor* fault isolation.

5. FDI PERFORMANCE ESTIMATION

To show the diagnostic characteristics brought by the application of the proposed FDI schemes to general aviation aircrafts, some numerical results obtained in the Matlab® and Simulink® environment are reported. The final performances that are achieved with the developed FDI schemes are finally reported. These performances are evaluated by means of extensive simulations applied to the aircraft simulation model. This section presents also some comparisons of the developed PM and NLGA FDI strategies with NN and UIKF FDI schemes.

The designed PM residual generator filters are fed by the 4 signals of the input vector $c(t)$ and the 9 signals of output vector $y(t)$ acquired from the simulation aircraft model previously described. In particular, a bank of 4 residual generator filters has been used to detect input sensor faults regarding the 4 input control variables. Obviously, the residual generator bank has been designed to be decoupled from the 3 component wind disturbance vector $d(t) = [w_u(t), w_v(t), w_w(t)]^T$. Regarding the NLGA residual generator filters, a bank of 4 residual generator filters has been used. However, the i–th NLGA residual generator is fed by one signal of the input vector $c(t)$, with $i = 1, \ldots, 4$. Analogously to the PM, the approximations of the NLGA synthesis nonlinear model are related to a particular steady–state flight condition.

The chosen single steady–state flight condition for the design both of the PM and of the NLGA residual generators is a coordinated turn characterised by the true–air–speed of 50 m/s, the curvature radius of 1000 m, the flight–path angle of 0°, the altitude of 330 m and the flap deflection of 0^o. This represents one of most general flight condition, due to the coupling of the longitudinal and lateral dynamics.

In order to assess the presented diagnosis techniques, different fault sizes have been simulated on each sensor. Single faults in the input sensors have been generated by producing abrupt (step) variations in the input signals $c(t)$. The residual signals indicate fault occurrence according to whether their values are lower or higher than the thresholds fixed in fault–free conditions. To summarise the performances of the PM FDI scheme, the minimal detectable step faults on the various input sensors are collected in Table 2. Regarding the NLGA FDI scheme, the minimal detectable faults concerning the input sensors are summarised in Table 3. The minimal detectable fault

Table 2. PM minimal detectable step input sensor faults.

Variable	Fault Size	Delay Time
δ_e	2^o	18 s
δ_a	3^o	6 s
δ_r	4^o	8 s
δ_{th}	2%	15 s

Table 3. NLGA minimal detectable input sensor faults.

Variable	Fault Size	Delay Time
δ_e	2^o	5 s
δ_a	2^o	3 s
δ_r	2^o	6 s
δ_{th}	6%	3 s

values in Table 2 and Table 3 are expressed in the unit of measure of the sensor signals. The detection delay times represent the worst case results, as they are evaluated by monitoring the slowest residual generator function.

The characteristics of the proposed PM and NLGA FDI schemes have been evaluated and compared also with respect to the UIKF scheme (Chen and Patton (1999)) and the NN technique (Korbicz et al. (2004)). In particular, a bank of UIKF has been exploited for diagnosing faults of the monitored process. The procedure recalled here requires the design of an UIKF bank and the basic scheme is the standard one: a set of measured variables of the system is compared with the corresponding signals estimated by filters to generate residual functions. The diagnosis has been performed by detecting the changes of UIKF residuals caused by a fault. The FDI input sensor scheme exploits a number of UIKF equal to the number of input variables. Each filter is designed to be insensitive to a different input sensor of the process and its disturbances (the so–called unknown inputs). Moreover, the considered UIKF bank was obtained by following the design technique described in (Chen and Patton (1999)) (Section 3.5, pp. 99–105), whilst the noise covariance matrices were estimated as described in (Simani et al. (2002)) (Section 3.3, pp. 70–74 and Section 4.6, pp. 130–131). Each of the 4 UIKF of the bank was de–coupled from both one input sensor fault and the wind gust disturbance component, thus providing the optimal filtering of the input–output measurement noise sequences.

On the other hand, a dynamic NN bank has been exploited in order to find the dynamic connection from a particular fault regarding the input sensors to a particular residual. In this case, the learning capability of NN are used for identifying the nonlinear dynamics of the monitored plant. The dynamic NN provides the prediction of the process output with an arbitrary degree of accuracy, depending on the NN structure, its parameters and a sufficient number of neurons. Once the NN has been properly trained, the residuals have been computed as difference between predicted and measured process outputs. The FDI is therefore achieved by monitoring residual changes. The NN FDI method exploits a bank of 4 time–delayed three–layers perceptrons NN with 15 neurons in the input layer, 25 neurons in the hidden layer and 1 neuron in the output layer. Each NN was designed to be insensitive to each input sensor fault, and the NN were trained in order to provide the optimal output prediction on the basis of the training pattern and target sequences (Korbicz et al. (2004)).

The performances of the different FDI schemes have been evaluated by considering a more complex aircraft trajectory. This closed trajectory consists of 4 steady–state flight conditions, *i.e.* 2 coordinated turns and 2 straight paths. The performed tests represent also a possible reliability and robustness experimental evaluation of the considered FDI techniques. In fact, in this case the diagnosis requires that the residual generators are robust with respect to the flight conditions that do not match the nominal trajectory used for the design.

As an example, Fig. 1 shows the 4 residual functions generated for the complete trajectory by the previously designed PM filter bank, which provided the results of Table 2 in the nominal flight condition. On the basis of the fault–free and faulty conditions represented in Fig. 1, this bank provides the correct isolation of the considered input sensor fault.

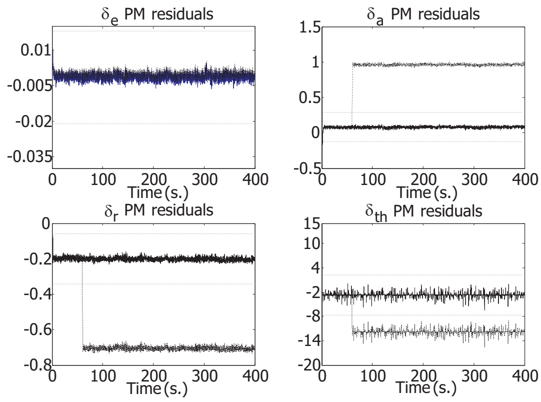

Fig. 1. PM residuals for the 1st input sensor FDI.

In particular, Fig. 1 represents the fault–free and the faulty residual signals. Horizontal lines show the levels of the fault–free thresholds. In the considered case, the fault has been generated on the 1st input sensor of the considered aircraft, starting at time $t = 60\,$s. The first residual function, as depicted in Fig. 1, provides also the isolation of the fault $f_c(t)$ regarding the 1st input sensor. In fact the residual for the the 1st input does not depend on the considered fault, since it has been designed to be insensitive to the related input signal.

The second example of Fig. 2 shows the 4 residual functions generated by the NLGA filter bank applied to the complete aircraft trajectory. The results achieved in the nominal flight condition are collected in Table 3. In Fig. 2, horizontal lines represent the FDI thresholds. Note that, due to the NLGA design technique presented in Section 3, only the 1st residual related to the δ_e signal of the filter bank is sensitive to a fault affecting the 1st input sensor.

Table 4 summarises the results obtained by considering the observers and filters (corresponding to the PM, NLGA, UIKF and NN) for the input sensor FDI, whose parameters have been designed and optimised for the steady–state coordinated turn represented by one reference flight condition of the complete trajectory. Table 4 reports the performances of the considered FDI techniques in terms

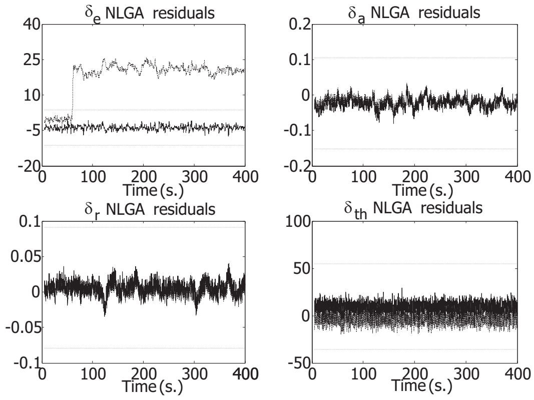

Fig. 2. NLGA residuals for the 1st input sensor FDI.

of the minimal detectable step faults on the various input sensors. The detection delay times reported in Table 4 represent the average delay time values among the different fault cases for the complete trajectory. Further experiment

Table 4. Performances of the FDI schemes.

Variable	**PM**	**NLGA**	**UIKF**	**NN**
δ_e	4^o	3^o	4^o	3^o
δ_a	5^o	3^o	5^o	4^o
δ_r	5^o	3^o	4^o	4^o
δ_{th}	7 %	10 %	11 %	12 %
Delay Time	28 s.	29 s.	31 s.	30 s.

results have been reported in the following of this section. They regard the performance evaluation of the developed FDI scheme with respect to modelling errors and measurement uncertainty. Extensive simulations are useful at this stage as the FDI performances depend on the residual error magnitude due to the model approximation as well as on the measured signal $c(t)$ and $y(t)$ errors.

As remarked above, the aircraft simulator is able to vary the reference trajectory and the properties of the signals used for modelling both the process and measurement errors. Due to the nature of the simulated model, the simulation analysis represents an experimental method for estimating the capabilities of the developed FDI scheme, when applied to the considered aircraft.

For this experimental analysis, some performance indices have been used and then evaluated on a number of simulation runs equal to 1000. This number of simulations is used to experimentally evaluate the False Alarm Rate (FAR), the Missed Fault Rate (MFR), True Detection Rate (TDR) and Mean Detection Delay (MDD). Table 5 summarises the results obtained by considering the PM dynamic filters for the input sensor FDI with the parameters optimised as described in Section 4 for a complete aircraft trajectory. The same analysis can be

Table 5. PM residual analysis.

Sensor	**FAR**	**MFR**	**TDR**	**MDD**
δ_e	0.002	0.003	0.997	27s
δ_a	0.001	0.001	0.999	18s
δ_r	0.002	0.003	0.997	25s
δ_{th}	0.003	0.002	0.998	35s

applied again to the residual generated by means of the

NLGA, NN and UIKF FDI schemes. The results are summarised in Tables 6, 7 and 8. Tables 5, 6, 7 and 8

Table 6. NLGA residual analysis.

Sensor	FAR	MFR	TDR	MDD
δ_e	0.003	0.004	0.996	30s
δ_a	0.002	0.002	0.998	15s
δ_r	0.001	0.001	0.999	23s
δ_{th}	0.004	0.003	0.997	32s

Table 7. NN residual analysis.

Sensor	FAR	MFR	TDR	MDD
δ_e	0.004	0.005	0.995	33s
δ_a	0.003	0.003	0.997	23s
δ_r	0.004	0.004	0.996	29s
δ_{th}	0.005	0.003	0.997	38s

Table 8. UIKF residual analysis.

Sensor	FAR	MFR	TDR	MDD
δ_e	0.003	0.004	0.996	26s
δ_a	0.002	0.002	0.998	17s
δ_r	0.001	0.002	0.998	26s
δ_{th}	0.004	0.003	0.997	37s

show how the proper design of the dynamic filters allows to achieve false alarm and missed fault rates less than 0.6%, detection and isolation rates bigger than 99.4%, with minimal detection and isolation delay times.

6. CONCLUSION

The paper provided the development and application of FDI techniques based on a PM scheme and on a NLGA method, respectively. The PM procedure led to residual generators optimising the trade–off between disturbance decoupling and fault sensitivity. The proposed NLGA relies on a two design steps, where the former is concerned with the structural decoupling of critical disturbances and modelling errors, whilst the latter regards the optimisation of the trade–off between the fault sensitivity and robustness with respect to further non critical disturbances and uncertainties. In particular, the optimisation procedure aimed to the robustness improvement is based on the $\mathcal{H}_-/\mathcal{H}_\infty$ approach which has been analytically developed. The PM and NLGA residual generators were tested by considering a nonlinear aircraft simulator model that takes into account also the wind gusts, the Dryden turbulence, the input–output sensors measurement errors, the engine and the servo actuators.

In order to verify the achievable performances of the approaches, the simulation results considered a typical aircraft reference trajectory consisting of several steady–state flight conditions, such as straight flight phases and coordinated turns. The effectiveness of the developed FDI schemes was shown by simulations and a comparison with widely used data–driven and model–based disturbance decoupling FDI schemes, such as NN and UIKF diagnosis methods, was provided. The properties of the proposed residual generators with respect to uncertainty, disturbances and measurement noise for the aircraft nonlinear model were experimentally investigated. Thus, the evaluation of the performance achievable are estimated by using extensive simulations.

Further works involve the analysis of the proposed FDI algorithms when applied to real flight data.

REFERENCES

Francesco Amato, Carlo Cosentino, Massimiliano Mattei, and Gaetano Paviglianiti. A direct/functional redundancy scheme for fault detection and isolation on an aircraft. *Aerospace Science and Technology*, 10(4):338–345, May 2006.

M. Bonfè, P. Castaldi, W. Geri, and S. Simani. Design and Performance Evaluation of Residual Generators for the FDI of an Aircraft. *International Journal of Automation and Computing*, 4(2):156–163, April 2007. DOI: 10.1007/s11633–007–0156–7.

Marcello Bonfè, Paolo Castaldi, Walter Geri, and Silvio Simani. Fault Detection and Isolation for On–Board Sensors of a General Aviation Aircraft. *International Journal of Adaptive Control and Signal Processing*, 20 (8):381–408, October 2006. Copyright 2006 John Wiley & Sons, Ltd. ISSN: 0890-6327.

P. Castaldi, W. Geri, M. Bonfè, and S. Simani. Nonlinear Actuator Fault Detection and Isolation for a General Aviation Aircraft. In IFAC, editor, *ACA2007 – 17th IFAC Symposium on Automatic Control in Aerospace*, volume CD–Rom, pages 1–6, Toulouse, France, June, 25–29 2007. IFAC ACA, IFAC.

J. Chen and R. J. Patton. *Robust Model–Based Fault Diagnosis for Dynamic Systems.* Kluwer Academic Publishers, 1999.

C. De Persis and A. Isidori. On the observability codistributions of a nonlinear system. In *Systems and Control Letters*, volume 40, pages 297–304, 2000.

C. De Persis and A Isidori. A geometric approach to non–linear fault detection and isolation. *IEEE Transactions on Automatic Control*, 45(6):853–865, June 2001.

J. Gertler. *Fault Detection and Diagnosis in Engineering Systems.* Marcel Dekker, New York, 1998.

M. Hou and R. J. Patton. An LMI approach to H_-/H_∞ fault detection observers. In *CONTROL'96*, pages 305–310, University of Exeter, UK, 1996. IEE.

Rolf Isermann. *Fault–Diagnosis Systems: An Introduction from Fault Detection to Fault Tolerance.* Springer–Verlag, 1st edition, November, 28 2005. ISBN: 3540241124.

J. Korbicz, J. M. Koscielny, Z. Kowalczuk, and W. Cholewa, editors. *Fault Diagnosis: Models, Artificial Intelligence, Applications.* Springer–Verlag, 1st edition, February, 12 2004. ISBN: 3540407677.

Andrès Marcos, Subhabrata Ganguli, and Gary J. Balas. An application of H_∞ fault detection and isolation to a transport aircraft. *Control Engineering Practice*, 13(1): 105–119, January 2005.

R. J. Patton, P. M. Frank, and R. N. Clark, editors. *Issues of Fault Diagnosis for Dynamic Systems.* Springer–Verlag, London Limited, 2000.

S. Simani, C. Fantuzzi, and R. J. Patton. *Model-based fault diagnosis in dynamic systems using identification techniques.* Advances in Industrial Control. Springer–Verlag, London, UK, first edition, November 2002. ISBN: 1852336854.

B. L. Stevens and F. L. Lewis. *Aircraft Control and Simulation.* John Wiley and Son, 2^{nd} edition, 2003.